

A Novel High Step-Up DC–DC Converter for Hybrid Renewable Energy System applied to Irrigation

¹G.Anjali, ²G.Madhavi

¹Mtech student, electrical and electronics engineering, P.V.P.Siddhartha institute of chnology,
Krishna, A.P, India

²Assistant professor, electrical and electronics engineering, P.V.P. Siddhartha institute of technology,
Krishna, A.P, India

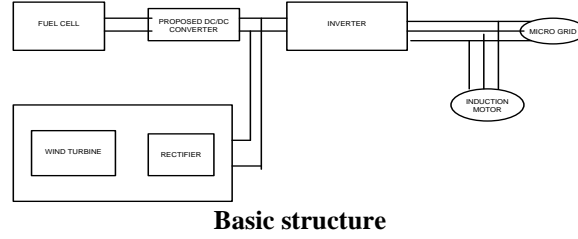
Abstract:- Large electric drives and utility applications require advanced power electronics converter to meet the high power demands. As a result, power converter structure has been introduced as an alternative in high power and medium voltage situations using Renewable energy sources (RES). This paper describes a new DC/DC converter with safety, high efficiency and high step up capabilities. This converter is best suited for Wind/Fuel cell(FC)based Induction Motor applications for pumping systems. The safety feature of this converter makes it friendly for the farmers to use it for irrigation and agriculture usages. The converter achieves high step-up voltage gain with appropriate duty ratio and low voltage stress on the power switches. Also, the energy stored in the leakage inductor of the coupled inductor can be recycled to the output. The maximum output voltage is determined by the number of the capacitors. The capacitors are charged in parallel and are discharged in series by the coupled inductor, stacking on the output capacitor. Thus, the proposed converter can achieve high step-up voltage gain with appropriate duty ratio and interfaced to induction motor through 9-level inverter and also energy fed to grid system when no load operation. The simulation results are obtained using MATLAB/SIMULINK software.

Keywords:- Coupled-inductor, high step-up voltage gain, switched capacitor, three phase inverter, grid connection.

I. INTRODUCTION

Renewable energy sources (RESs) have experienced a rapid growth in the last decade due to technological improvements, which have progressively reduced their costs and increased their efficiency at the same time [1]. Moreover, the need to depend less on fossil fuels and to reduce emissions of greenhouse gases, requires an increase of the electricity produced by RESs. This can be accomplished mainly by resorting to wind and photovoltaic generation, which, however, introduces several problems in electric systems management due to the inherent nature of these kinds of RESs [2]. In fact, they are both characterized by poorly predictable energy production profiles, together with highly variable rates. As a consequence, the electric system cannot manage these intermittent power sources beyond certain limits, resulting in RES generation curtailments and, hence, the RES penetration levels are lower than expected. Here front-end DC-DC converter is required for conversion of energy from one stage to another and interfaced to grid/load through inverter topology.

The DC-DC boost converter is used for voltage step-up applications, and in this case this converter will be operated at extremely high duty ratio to achieve high step-up voltage gain [1],[2]. However, the voltage gain and the efficiency are limited due to the constraining effect of power switches, diodes, and the equivalent series resistance (ESR) of inductors and capacitors. Based on the structure a switched capacitor (SC) converter is one of the good solutions to low power and high gain DC-DC conversion. The advantage is that this kind of SC converter uses semiconductor switches and capacitors only. However, most SC circuits have a voltage gain proportional to the number of pumping capacitors. Generally speaking, high step-up converter is used for this application which requires high voltage gain, and efficiency [5], [6]. To achieve high step-up voltage gain, many converters have been proposed. Some converters effectively combined both boost and flyback converters as one and other different converter combinations are developed to carry out high step-up volt-age gain by using the coupled-inductor technique. High voltage gain is restricted by the voltage stress on the active switch. But in case of coupled inductor technique the energy of the leakage inductor can be recycled that will reduce the voltage stress on active switch. This leads the coupled inductor technique more successful.



This paper proposes a novel high step-up voltage gain converter with 9-level inverter fed induction drive for irrigation system with good advantages. The proposed converter uses the coupled-inductor and switched-capacitor techniques. The coupled inductor is operated as transformer in flyback and forward converters. Thus, the capacitors on the output-stacking are charged in parallel and are discharged in series to achieve high step-up voltage gain.

II. OPERATING PRINCIPLE OF THE PROPOSED CONVERTER

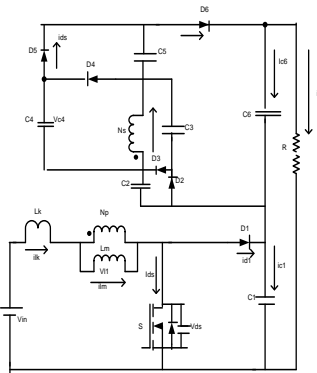


Fig. 1. Circuit configuration of the proposed converter.

Fig.1 shows the circuit topology of the proposed converter. The equivalent circuit model of the coupled inductor includes the magnetizing inductor L_m , leakage inductor L_k and an ideal transformer. This converter consists of one power switch, six diodes and six capacitors. The leakage-inductor energy of the coupled inductor is recycled to the capacitor C_1 , and thus the voltage across the switch S can be clamped. Also, the voltages across the capacitors C_2 , C_3 , C_4 , and C_5 can be adjusted by the turn's ratio of the coupled inductor. The voltage level of the switch is reduced significantly and low conducting resistance $R_{ds(on)}$ of the switch can be used. Thus, the efficiency of the proposed converter can be increased and high step-up voltage gain can be achieved. When switch S is turned on, dc source V_{in} charges leakage inductor L_k , magnetic inductor L_m and the coupled inductor induced voltage V_{L2on} on the secondary-side. Voltages V_{L2} and V_{c4} connected in series to charge capacitor C_5 . Meanwhile, Voltages V_{L2} and V_{c3} connected in series to charge capacitor C_2 . Thus, two capacitors C_2 and C_5 are charge in parallel. When switch S is turned off, the energy of leakage inductor L_k is released to output capacitor C_1 directly and magnetic energy of L_m released by the coupled inductor. The induced voltage V_{L2on} on the secondary-side of coupled inductor charges capacitors C_3 and C_4 in parallel. Also, voltages V_{L2} , V_{c2} , and V_{c5} are connected in series to charge output capacitor C_6 . The output voltage is stacked by capacitors C_1 and C_6 . The high step-up voltage gain is achieved. The energy of leakage inductor is sent to output. The voltage stress of main switch is clamped. To simplify the circuit analysis, the following conditions are assumed.

- 1) Capacitors C_1 – C_6 are large enough. Thus, V_{c1} – V_{c6} are considered as constant in one switching period.
- 2) The power devices are ideal, but the parasitic capacitor of the power switch is considered.
- 3) The coupling-coefficient of the coupled-inductor k is equal to $L_m/(L_m+L_k)$ and the turns ratio of the coupled-inductor n is equal to N_s/N_p . The proposed converter operating in continuous conduction mode (CCM) and discontinuous conduction mode (DCM) are analyzed as follows.

A. CCM Operation

Based on the above assumptions, Fig. 2 illustrates the typical waveforms and respective figures shows the topological stages of the proposed converter. The operating modes are described as follows.

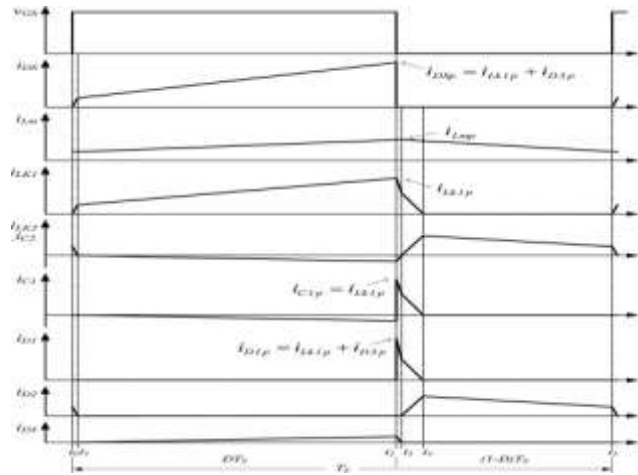


Fig.2.waveforms of the proposed converter at CCM operation

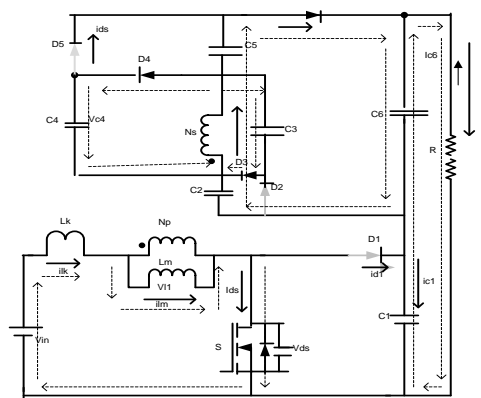


Fig.3Current-flow path in Mode I during CCM operation

Mode I [t₀,t₁]: During this time interval, S is turned on. Diodes D1, D2, and D5 are turned off, and D3, D4, and D6 are turned on. The current-flow path is shown in Fig. 3. The voltage of primary-side is $V_{in} = v_{Lk} + V_{L1}$. Thus, leakage inductor Lk and magnetic inductor Lm is charged by dc-source V_{in} . The primary current i_{Lk} increases linearly. Due to leakage inductor Lk, the secondary-side current is decreases linearly. Secondary side voltage V_{L2} , V_{c2} , and V_{c5} are connected in series to charge output capacitor C6 and to provide the energy to load R. Because i_{Lk} decreases linearly, the reverse recovery problem of the diode is alleviated. When current becomes zero at $t=t_1$, this operating mode is ended.

Mode II [t₁,t₂]: During this time interval, S is still turned on. Diodes D1, D3, D4, and D6 are turned off, and D2 and D5 are turned on. The current-flow path is shown in Fig. 4. The magnetizing inductor Lm is charged by dc-source V_{in} .

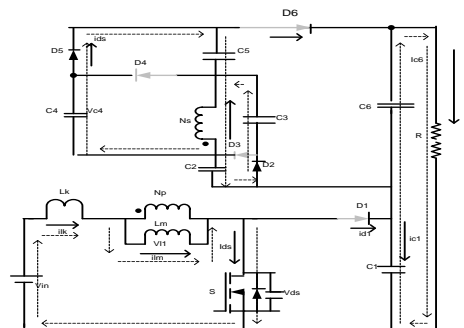


Fig. 4. Current-flow path in Mode II during CCM operation

The coupled inductor induces voltage V_{L2} on the secondary-side. Voltage V_{L2} which is connecting V_{C3} in series and connecting V_{C4} in series charge C2 and C5 in parallel. A part of the energy of dc-source V_{in} is transferred to capacitors C2 and C5 via the coupled inductor. Also, the energies of C3 and C4 are transferred to capacitors C2 and C5 together. Meanwhile, voltages V_{c2} and V_{c5} are approximately equal to $nV_{in} + V_{c3}$. The

output capacitor and $C1$ and $C6$ provides its energy to load R . This operating mode is ended when switch S is turned off at $t=t_2$.

Mode III [t_2, t_3]: During this time interval, S is turned off. Diodes $D1, D3, D4,$ and $D6$ are turned off, and $D2$ and $D5$ are turned on. The current-flow path is shown in Fig. 5. The energies of leakage inductor L_k and magnetizing inductor L_m are released to the parasitic capacitor C_{ds} of switch S . Capacitors $C2$ and $C5$ are charged by dc-source V_{in} . Output capacitors $C1$ and $C6$ provide energy to load R . When the capacitor voltage V_{c1} is equal to $V_{in} + V_{ds}$ at $t=t_3$, diode $D1$ is conducted and this operating mode is ended.

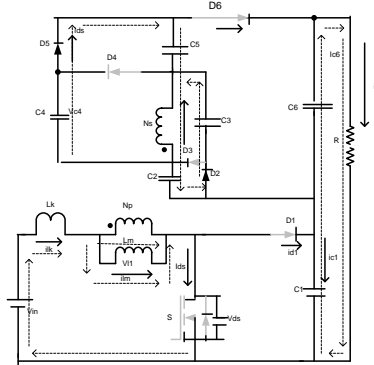


Fig.5. Current-flow path in Mode III during CCM operation

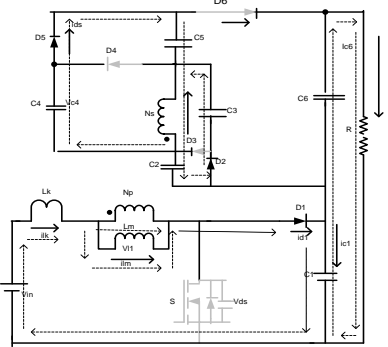


Fig. 6. Current-flow path in Mode IV during CCM operation

Mode IV [t_3, t_4]: During this time interval, S is turned off. Diodes $D1, D2,$ and $D5$ are turned on, and $D3, D4,$ and $D6$ are turned off. The current-flow path is shown in Fig. 6. The energies of leakage inductor L_k and magnetizing inductor L_m is released to capacitor $C1$. Thus, the voltage across the switch is clamped at V_{c1} . The current i_{Lk} decreases quickly. The secondary-side voltage of the coupled inductor V_{L2} charges capacitors $C2$ and $C5$ in parallel until the secondary-side current is equals zero. Thus, diodes $D2$ and $D5$ are cut off at $t=t_4$. This operating mode is ended.

Mode V [t_4, t_5]: During this time interval, S is turned off. Diodes $D1, D3, D4,$ and $D6$ are turned on, and $D2$ and $D5$ are turned off. The current-flow path is shown in Fig. 7. The energies of leakage inductor L_k and magnetizing inductor L_m is released to capacitor $C1$. Capacitors $C3$ and $C4$ are charged in parallel by the magnetizing inductor energy via coupled inductor. Simultaneously, secondary-side voltage V_{L2} is connected with V_{c2} and V_{c5} in series and charges output capacitor $C6$. This operating mode is ended when capacitor $C1$ starts to discharge at $t=t_5$.

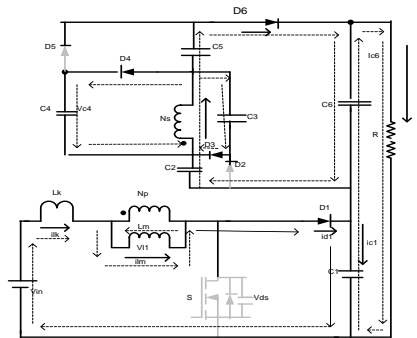


Fig.7. Current-flow path in Mode V during CCM operation

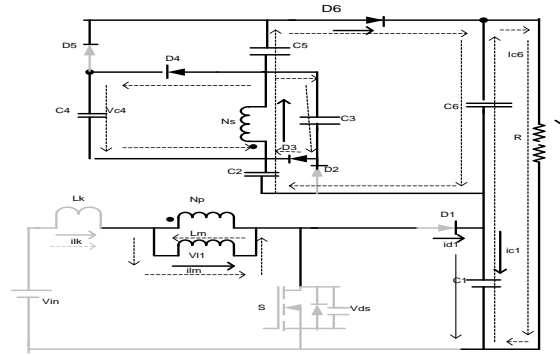


Fig.8. Current-flow path in Mode VI during CCM

Mode VI[t_5, t_6]: During this time interval, S is still turned off. Diodes D3, D4, and D6 are turned on, and D1, D2, and D5 are turned off. The current-flow path is shown in Fig.8. The magnetizing energy of L_m is transferred to capacitors C3 and C4 by coupled inductor. Thus, two capacitors are charged in parallel. Also, VL2, Vc2 and Vc5 are connected in series and charge capacitor C6. This mode is ended at $t=t_6$ when S is turned on at the beginning of the next switching period.

B. DCM Operation

To simplify the analysis of DCM operation, the leakage inductor L_k of the coupled-inductor is neglected. Fig. 9 shows typical waveforms of the proposed converter operated in DCM. The operating modes are described as follows.

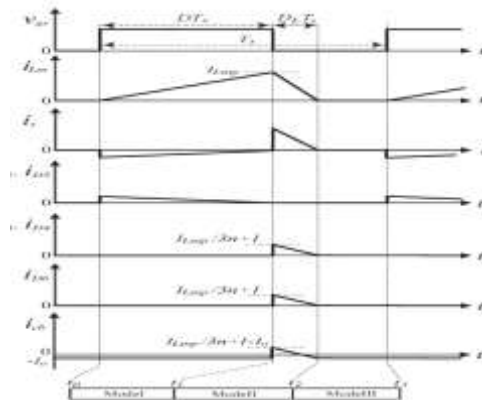


Fig.9.waveforms of the proposed converter at DCM operation

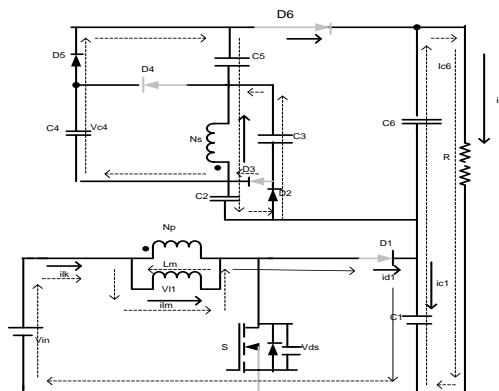


Fig.10. Current-flow path in Mode I during DCM

Mode I[t_0, t_1]: During this time interval, S is turned on. The current-flow path is shown in Fig.10. The energy of dc source V_{in} charges magnetizing inductor L_m . Thus, i_{Lm} is increased linearly. Also, the secondary side of the coupled inductor is connected series with capacitor C3 or C4 and releases their energies to charge capacitors C2 and C5 in parallel. Output capacitors C1 and C6 provide energy to load R. This mode is ended when S is turned off at $t=t_1$.

Mode II [t1,t2]: During this time interval, S is turned off. The current-flow path is shown in Fig.11. The energies of dc source V_{in} and magnetizing inductor L_m are transferred to capacitors C_1 and load R. Similarly, capacitors C_2 and C_5 are discharged in series with dc source V_{in} and magnetizing inductor L_m to capacitor C_6 and load R. Meanwhile, the energy of magnetizing inductor L_m is transferred to capacitors C_3 and C_4 by coil N_s . This mode is ended when the energy stored in L_m is empty at $t=t_2$.

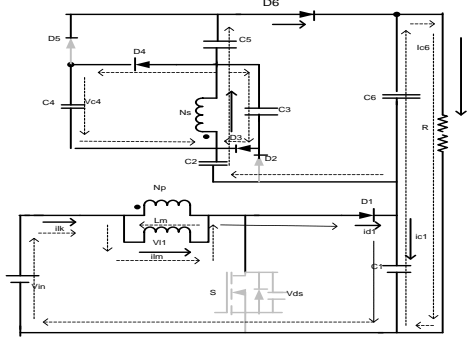


Fig.11. Current-flow path in Mode III during DCM

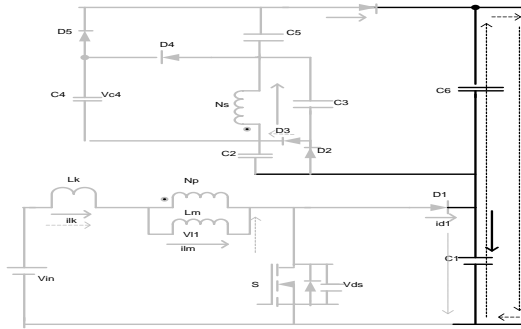


Fig.12. Current-flow path in Mode II during DCM operation

Mode III [t2,t3]: During this time interval, S is turned off. The current-flow path is shown in Fig.12. Since the energy stored in L_m is empty, the energy stored in C_1 and C_6 are discharged to load R. This mode is ended when S is turned on at $t=t_3$.

III. STEADY-STATE ANALYSIS OF PROPOSED CONVERTER OF CCM OPERATION

To simplify the steady-state analysis, only modes II and IV are considered for CCM operation and the leakage

Inductances on the secondary and primary sides are neglected. The equations are following

$$V_{ln} = V_{in} \quad (1)$$

$$V_{N2} = nV_{in} \quad (2)$$

$$V_{lm} = -V_{c1} \quad (3)$$

$$V_{N2} = -V_{c2} \quad (4)$$

Applying a volt-second balance on the magnetizing inductor L_m yields

$$\int_0^{DTs} (V_{in}) dt + \int_{DTs}^{Ts} (-V_{c1}) dt = 0 \quad (5)$$

$$\int_0^{DTs} (nV_{in}) dt + \int_{DTs}^{Ts} (-V_{c2}) dt = 0 \quad (6)$$

From which the voltage across capacitors C_1 and C_2 are obtained as follows:

$$V_{c1} = \frac{D}{1-D} V_{in} \quad (7)$$

$$V_{c2} = \frac{nD}{1-D} V_{in} \quad (8)$$

During mode II, the output voltage $V_0 = V_{in} + V_{N2} + V_{C2} + V_{C1}$
 Becomes

$$V_0 = V_{in} + nV_{in} + \frac{nD}{1-D}V_{in} + \frac{D}{1-D}V_{in} \quad (9)$$

The DC voltage gain M_{CCM} can be found as follows:

$$M_{CCM} = \frac{V_0}{V_{in}} = \frac{1+n}{1-D}$$

Voltage gain M_{CCM} as function of duty ratio D of the proposed converter.

IV. HYBRID GENERATION SCHEME WITH INVERTER MODEL

Hybrid renewable energy systems becoming popular for remote area power generation applications due to advances in technologies and subsequent rise in prices of petroleum products. A hybrid energy system usually consists of two or more renewable energy sources used together to provide increased system efficiency as well as greater balance in energy supply. A hybrid energy system is Fuel cells coupled with a wind turbine. Hybrid energy systems often times yield greater economic and environmental returns than wind, solar, geothermal or regeneration stand-alone systems by themselves. For example, let us consider a load of 100% power supply and there is no renewable system to fulfill this need, so two or more renewable energy system can be combined. 60% from a wind energy system and the balance from fuel cells. Thus combining all these renewable energy systems may provide 100% of the power and energy requirements for the load, such as a home or business.

A. Wind Energy System

Wind turbines transform wind energy into electricity. The wind is a highly variable source, which cannot be stored. The principle of operation of a wind turbine is characterized by two conversion steps. First the rotor extract the kinetic energy of the wind, changing it into mechanical torque in the shaft; and in the second step the generation system converts this torque into electricity. In the most common system, the generator system gives an AC output voltage that is dependent on the wind speed. As wind speed is variable, the voltage generated has to be transferred to DC and back again to AC with the aid of inverters. However, fixed speed wind turbines are directly connected to grid.

B. Fuel Cell System

The fuel cells are electrochemical devices that convert chemical energy directly into electrical energy by the reaction of hydrogen from fuel and oxygen from the air without regard to climate conditions, unlike hydro or wind turbines and photovoltaic array. Fuel cells are different from batteries in that they require a constant source of fuel and oxygen to run, but they can produce electricity continually for as long as these inputs are supplied. Thus, the fuel cells are among the most attractive DGs resources for power delivery. However, batteries need to be placed in parallel or in series with the fuel cells as a temporary energy storage element to support during startup or sudden load changes because fuel cells cannot immediately respond to such abrupt load changes. Generally, fuel cells produce dc voltage outputs, and it keeps on varying with the load. So they are always connected to electric power networks through power conditioning units such as DC/DC and DC/AC to maintain the voltage constant or to stabilize the voltage.

C. Inverter Module

Switch-mode dc-to-ac converters used in ac power supplies and ac motor drives where the objective is to produce a sinusoidal ac output whose magnitude and frequency can both be controlled. High power and high-voltage conversion systems have become very important issues for the power electronic industry handling the large ac drive and electrical power applications at both the transmission and distribution levels. The main purpose of these topologies is to provide a three-phase voltage source, where the amplitude, phase, and frequency of the voltages should always be controllable. Although most of the applications require sinusoidal voltage waveforms (like ASDs, UPSs,) arbitrary voltages are also required in some emerging applications. The standard three-phase VSI topology is shown in Fig. 13 and the eight valid switch states are given in Table I. As in single-phase VSIs, the switches of any leg of the inverter (S_1 and S_4 , S_3 and S_6 , or S_5 and S_2) cannot be switched on simultaneously because this would result in a short circuit across the dc link voltage supply.

Similarly, in order to avoid undefined states in the VSI, and thus undefined ac output line voltages, the switches of any leg of the inverter cannot be switched off simultaneously as this will result in voltages that will depend upon the respective line current polarity of the eight valid states, two of them produce zero ac line voltages. In this case, the ac line currents freewheel through either the upper or lower components. The remaining states (1 to 6 in Table I) produce non-zero ac output voltages [5].

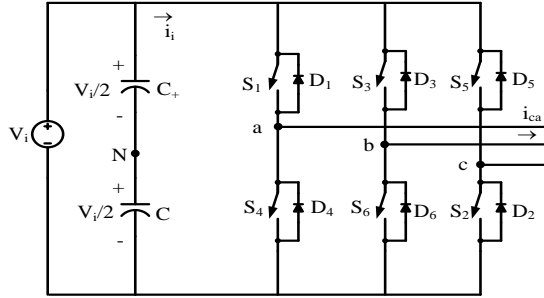


Fig. 13 Three-Phase VSI Topology

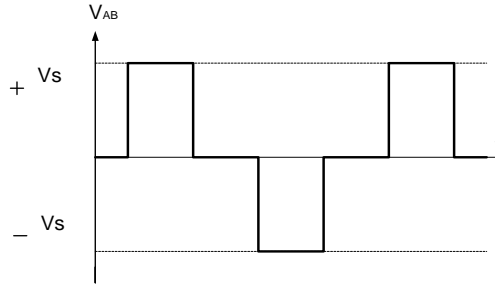


Fig. 14 Output waveform of Full Bridge Inverter

In order to generate a given voltage waveform, the inverter moves from one state to another. The selection of the states in order to generate the given waveform is done by the modulating technique that should ensure the use of only the valid states.

Table I Switching pattern of Three phase VSI

Conducting Switches	V_{AB}	V_{BC}	V_{CA}
S_1, S_2, S_6	$+V_s$	0	$-V_s$
S_2, S_3, S_1	0	V_s	$-V_s$
S_3, S_4, S_2	$-V_s$	V_s	0
S_4, S_5, S_3	$-V_s$	0	V_s
S_5, S_6, S_4	0	$-V_s$	V_s
S_6, S_1, S_5	V_s	$-V_s$	0

V. MATLAB MODELING AND SIMULATION RESULTS

In this paper Simulation is carried out in two different cases, they are

- 1) A Novel Improved Operation of High Step up DC/DC Converter.
- 2) A Standalone System with Hybrid Generation Scheme for Irrigation Applications.

Case 1: Proposed Novel Improved Operation of High Step up DC/DC Converter

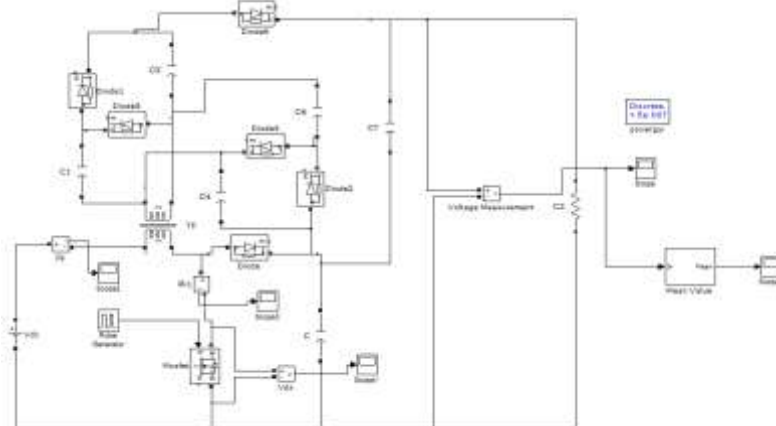


Fig.15 MATLAB/Simulink Model of Proposed Novel Improved Operation of High Step up DC/DC Converter

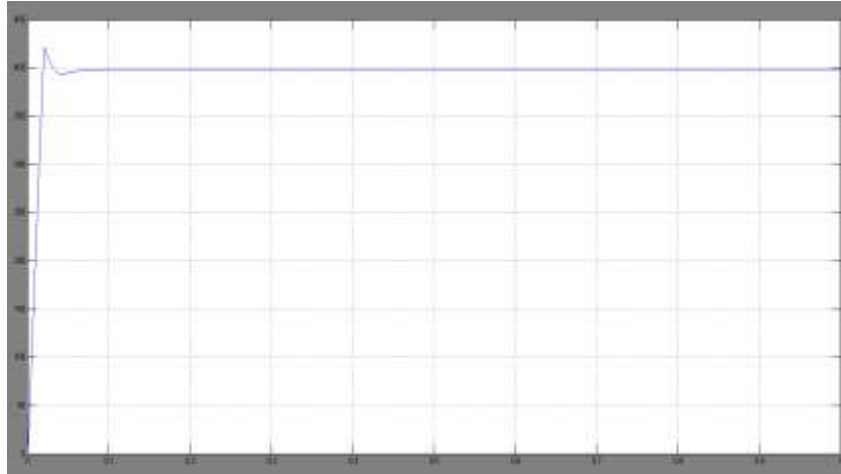


Fig.16 Output Voltage

Fig.16 Output Voltage of Proposed Novel Improved Operation of High Step up DC/DC Converter.

In this model the given low voltage DC voltage i.e. 45V is step up to high DC voltage i.e. 800V with the help of coupled inductor technique

Case 2: A Standalone System with Hybrid Generation Scheme for Irrigation Applications

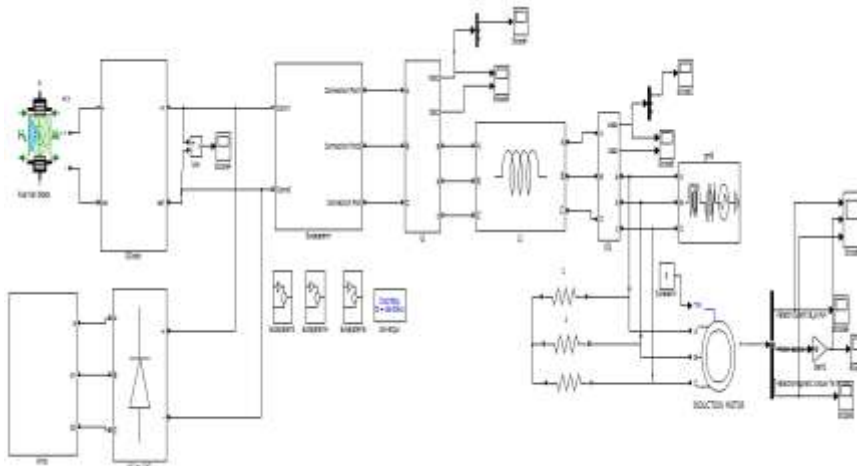


Fig.18 Matlab/Simulink Model of Standalone System with Hybrid Generation Scheme for Irrigation Applications

The above figure (fig18) shows simulation diagram of proposing System of fuel cell and wind turbine, interleaved high step-up dc-dc converter three phase inverter and grid connection. In this model the output DC voltages from fuel cell and wind turbines are fed to the grid and induction motor through three phase inverter (DC/AC) whenever the power is required for irrigation then the output of the inverter is given as an input to the induction motor otherwise it will be fed to the grid. Here 840V from renewable energy system is given as input to the inverter then this DC voltage is converted to 400v AC and that is fed to the grid and induction motor.

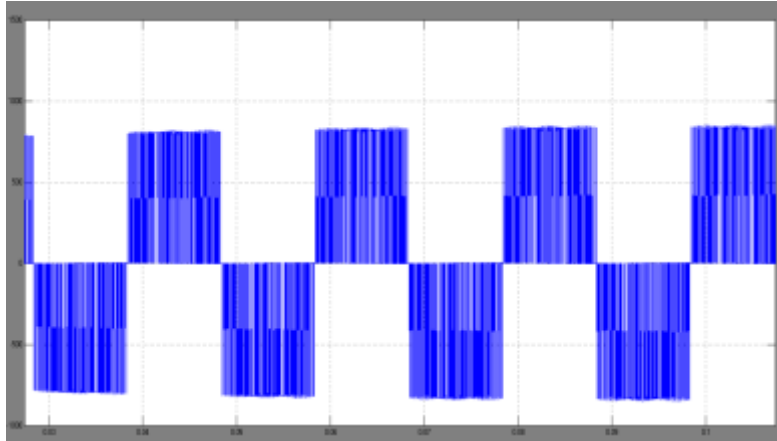


Fig.19 Three Level Output Voltage

Figure 19 shows the output voltage for three phase three level inverter. The obtained voltage is 800V

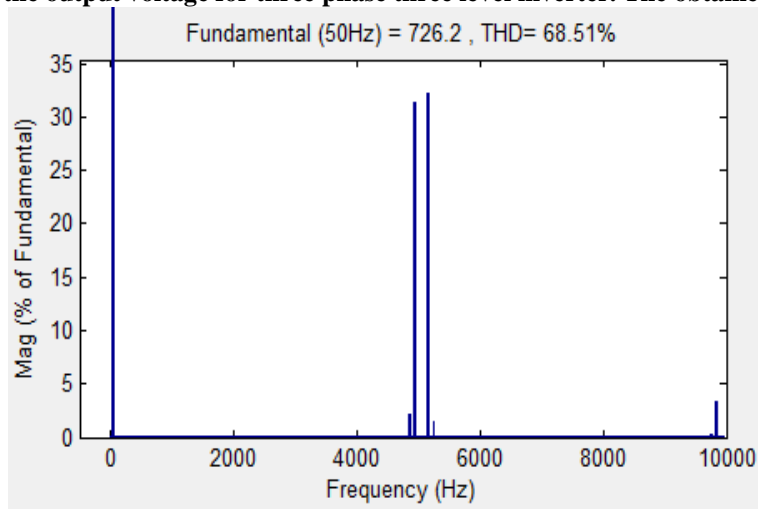


Fig.20 FFT Analysis of Grid Interfaced 3-Level Inverter Topology

Fig 19 shows the output voltage for three phase three level inverter. The obtained output voltage is 800V
Fig.20 shows the FFT Analysis of Grid Interfaced 3-Level Inverter Topology, the THD attained is 68.51%.

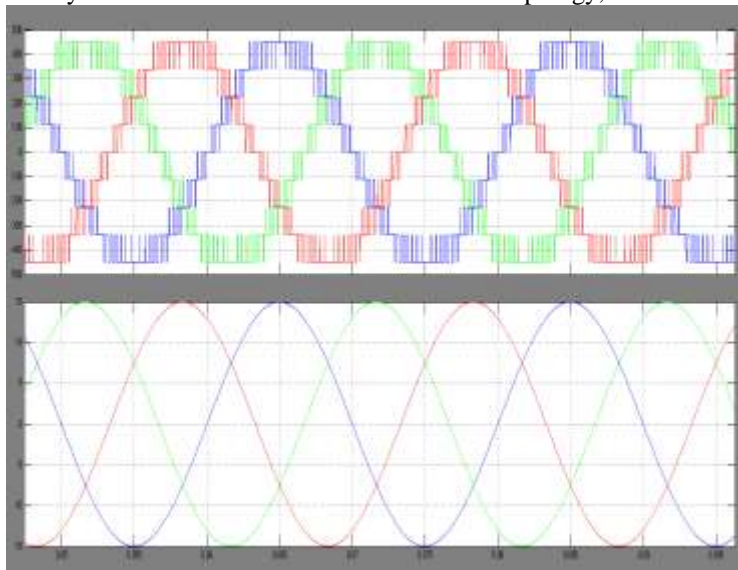


Fig.21 Nine Output Voltage & Current

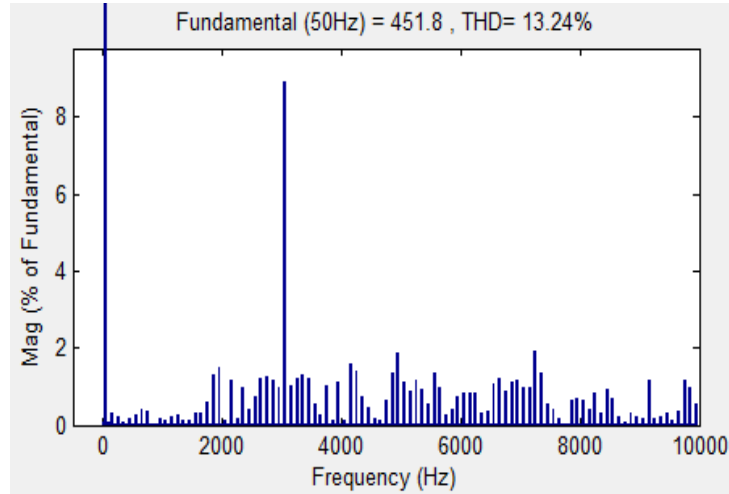


Fig.22 FFT Analysis of Grid Interfaced 9-Level Inverter Topology

Fig 21 shows the output voltage for three phase nine level inverter. The obtained output voltage is 800V. Fig.22 shows the FFT Analysis of Grid Interfaced 9-Level Inverter Topology, attained is 13.24%. When 3 level and 9 level inverter are compared With the increase in the number of levels, (Total Harmonic distortion) THD drastically reduces and also minimize the load side filter value.

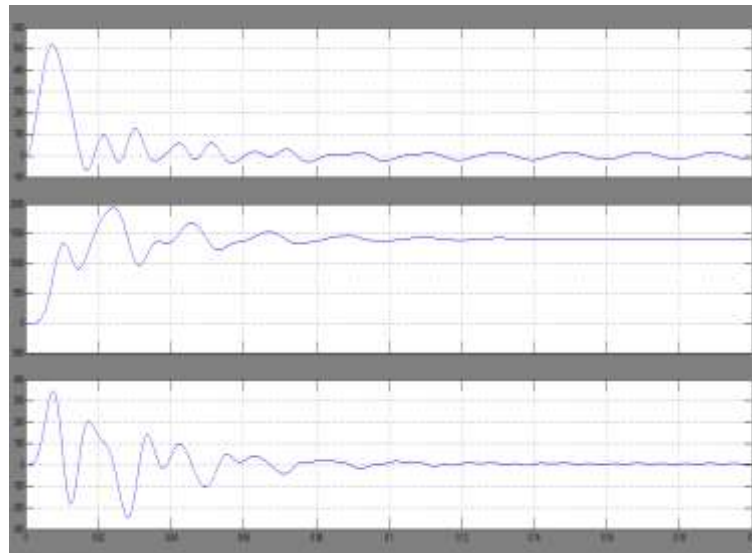


Fig.23 Stator Current, Speed, Electromagnetic Torque

Fig.23 shows the Stator Current, Speed, and Electromagnetic Torque of Standalone System with Hybrid Generation Scheme for Irrigation Applications.

VI. CONCLUSION

This new proposing system is an effective high step up interleaved dc-dc converter with grid connection system produces three phase output voltage. Utilization of renewable energy resources with advancement in power electronic technology, it has been recognized as an important renewable energy resource because it is clean, abundant and pollution free. This paper has proposed a 9-level inverter fed Induction motor drive for irrigation application and interfaced to grid when no load operation with co-generation system, high efficiency and high step-up dc-dc converter with the coupled inductor and switched capacitors techniques applications to RES. The proposed converter act as active component interfacing this RES system to grid connected system and have passive components without extra winding stage, and uses capacitors charged in parallel and discharged in series with a coupled inductor to achieve high step-up voltage gain. The steady-state analyses of voltage gain discussed and simulation results also presented. By using hybrid generation scheme, the system attains low voltage fluctuations, maintain high power density, improve grid stability, and achieve high reliability.

REFERENCES

- [1]. Yi-Ping Hsieh, Jiann-Fuh Chen, Member, IEEE, Tsorng-Juu Liang, Senior Member, IEEE, and Lung-Sheng Yang Novel High Step-Up DC–DC Converter with Coupled-Inductor and Switched-Capacitor Techniques.
- [2]. V. Scarpa, S. Buso, and G. Spiazzi, “Low-complexity MPPT technique exploiting the PV module MPP locus characterization,” *IEEE Trans. Ind. Electron.*, vol. 56, no. 5, pp. 1531–1538, May 2009.
- [3]. C. L. Chen, Y. Wang, J. S. Lai, Y. S. Lee, and D. Martin, “Design of parallel inverters for smooth mode transfer microgrid applications,” *IEEE Trans. Power Electron.*, vol. 25, no. 1, pp. 6–15, Jan. 2010.
- [4]. A. Timbus, M. Liserre, R. Teodorescu, P. Rodriguez, and F. Blaabjerg, “Evaluation of current controllers for distributed power generation systems,” *IEEE Trans. Power Electron.*, vol. 24, no. 3, pp. 654–664, Mar. 2009.
- [5]. R. J. Wai, C. Y. Lin, C. Y. Lin, R. Y. Duan, and Y. R. Chang, “High efficiency power conversion system for kilowatt-level stand-alone generation unit with low input voltage,” *IEEE Trans. Ind. Electron.*, vol. 55, no. 10, pp. 3702–3714, Oct. 2008.
- [6]. B. Axelrod, Y. Berkovich, and A. Ioinovici, “Transformerless dc-dc converters with a very high dc line-to-load voltage ratio,” in *Proc. IEEE ISCAS*, 2003, pp. III-435–III-438.
- [7]. K. C. Tseng and T. J. Liang, “Analysis of integrated boost-flyback stepup converter,” *Proc. Inst. Elect. Eng.-Elect. Power Appl.*, vol. 152, no. 2, pp. 217–225, Mar. 2005.
- [8]. R. J. Wai and R. Y. Duan, “High-efficiency dc/dc converter with high voltage gain,” *Proc. Inst. Elect. Eng.-Elect. Power Appl.*, vol. 152, no. 4, pp. 793–802, Jul. 2005.
- [9]. R. J. Wai and R. Y. Duan, “High step-up converter with coupled-inductor,” *IEEE Trans. Power Electron.*, vol. 20, no. 5, pp. 1025–1035, Sep. 2005.
- [10]. R. J. Wai, L. W. Liu, and R. Y. Duan, “High-efficiency voltage-clamped dc-dc converter with reduced reverse-recovery current and switch-voltage stress,” *IEEE Trans. Ind. Electron.*, vol. 53, no. 1, pp. 272–280, Feb. 2005.
- [11]. J. W. Baek, M. H. Ryoo, T. J. Kim, D. W. Yoo, and J. S. Kim, “High boost converter using voltage multiplier,” in *Proc. IEEE IECON*, 2005, pp. 567–572.
- [12]. G. V. T. Bascope, R. P. T. Bascope, D. S. Oliveira, Jr., S. A. Vasconcelos, F. L. M. Antunes, and C. G. C. Branco, “A high step-up dc-dc converter based on three-state switching cell,” in *Proc. IEEE ISIE*, 2006, pp. 998–1003.
- [13]. S. V. Araujo, R. P. Torrico-Bascope, and G. V. Torrico-Bascope, “Highly efficient high step-up converter for fuel-cell power processing based on three-state commutation cell,” *IEEE Trans. Ind. Electron.*, vol. 57, no. 6, pp. 1987–1997, Jun. 2010